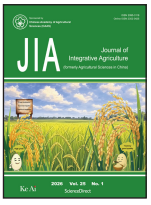
Journal of Integrative Agriculture 2026, 25(1): 157–165

Available online at ScienceDirect

Journal of Integrative Agriculture



RESEARCH ARTICLE

Identification of *Fusarium cugenangense* as a causal agent of wilt disease on *Pyrus pyrifolia* in China

Chaohui Li[1], Xiaogang Li[2], Weibo Sun[1], Yanan Zhao[3], Yifan Jia[1], Chenyang Han[3], Peijie Gong[1], Shutian Tao[3], Yancun Zhao[1#], Fengquan Liu[1, 4#]

[1] *Institute of Plant Protection, Jiangsu Academy of Agricultural Sciences/Jiangsu Key Laboratory for Food Quality and Safety-State Key Laboratory Cultivation Base of Ministry of Science and Technology, Nanjing 210014, China*
[2] *Institute of Pomology, Jiangsu Academy of Agricultural Sciences, Nanjing 210014, China*
[3] *State Key Laboratory of Crop Genetics and Germplasm Enhancement/College of Horticulture, Nanjing Agricultural University, Nanjing 210095, China*
[4] *Department of Plant Pathology, College of Agriculture, Guizhou University, Guiyang 550025, China*

Highlights

- *Fusarium cugenangense* is identified as a novel causal agent of pear wilt in China.
- Systemic infection is demonstrated *via* GFP-labeling and ultrastructural analysis.

Abstract

In recent years, an unusual wilt disease affecting *Pyrus pyrifolia* has been observed in various regions of Jiangsu, China. This disease originates from the roots and progresses with distinctive browning patterns along vascular tissues, even extending over two meters above the ground. These symptoms set it apart from recognized pear diseases and typically lead to the death of affected trees within the same or the following year. Furthermore, this disease exhibits a tendency to spread to neighboring trees even after the removal of affected trees, presenting a substantial threat to pear production. To ascertain the causative agent, the present study encompassed pathogen isolation, morphological and molecular identification, as well as validation experiments adhering to Koch's postulates. The fungal isolates obtained were identified as *Fusarium cugenangense* based on characteristics of the colonies and conidia, in addition to a phylogenetic analysis using DNA sequences of the translation elongation factor 1-alpha (*tef1*), calmodulin (*CaM*), and RNA polymerase second largest subunit (*rpb2*) genes. Pathogenicity of the isolated *F. cugenangense* on pear was confirmed by artificial inoculation. By introducing GFP-labeled pathogens into the roots, colonization in stem and leaf tissues was observed *via* fluorescence microscopy and transmission electron microscopy. Furthermore, these pathogens were successfully reisolated from stems and foliage, conclusively providing evidence of systemic infection within the pear plants. To the best of our knowledge, this is the first report of *F. cugenangense* causing pear wilt disease in China.

Keywords: *Fusarium cugenangense*, pear, root rot, necrosis, infection

1. Introduction

Pear trees (*Pyrus* spp.) hold global significance as fruit-bearing trees, serving multiple purposes ranging from fresh consumption to processing and commercial trade (Wu *et al*. 2018). These traditional cultivars are of great nutritional, health, and economic value, especially in China (Sun *et al*. 2023). However, the growth of pear trees is persistently afflicted by a multitude of diseases. Various pear cultivars worldwide have reported afflictions by at least 13 fungal diseases, including blue mold, gray mold, bitter rot, black spot, brown rot, bull's eye rot, pink mold rot, powdery mildew, *Rhizopus* rot, scab, side rot, and sooty blotch (Sardella *et al*. 2016). These diseases are categorized based on their location, mainly as leaf, fruit, or root diseases. While root diseases are less prevalent than leaf and fruit diseases, they significantly impact tree vigor, causing branch necrosis, and

Received 16 November 2023; Received in revised form 20 December 2023; Accepted 1 January 2024; Available online 29 February 2024
Chaohui Li, E-mail: chaohuili@yeah.net; #Correspondence Yancun Zhao, E-mail: zhaoyc27@126.com; Fengquan Liu, Tel: +86-25-84390277, E-mail: fqliu20011@sina.com

© 2026 CAAS. Publishing services by Elsevier B.V. on behalf of KeAi Communications Co. Ltd. This is an open access article under the CC BY-NC-ND license (http://creativecommons.org/licenses/by-nc-nd/4.0/). Peer review under responsibility of Editorial Board of *Journal of Integrative Agriculture*.
doi: 10.1016/j.jia.2024.02.018

in severe cases, complete tree mortality. These diseases pose a substantial threat to the vitality and yield potential of fruit-bearing trees, resulting in reduced harvests and overall orchard health decline (Bodah 2017).

Pear trees are susceptible to several root diseases caused by fungi, such as *Phytophthora* root rot from *Phytophthora cactorum* and *Phytophthora palmivora*, *Armillaria* root rot caused by *Amillariella tabescens*, and *Rhizoctonia* root rot triggered by *Rhizoctonia solani* (Wang *et al*. 2013; Sardella *et al*. 2016; Türkölmez *et al*. 2016). A recent addition to this list is *Fusarium* root rot in Asian pears, linked to *Fusarium solani* in China, as reported by Zhu *et al*. (2017). Upon infection by these pathogenic fungi, pear trees typically exhibit various symptoms, including reduced growth and vigor, leaf yellowing or chlorosis, premature fruit drop, and, ultimately, tree collapse or fatality. Apart from the aforementioned diseases, there are currently no reported cases of new pear tree root diseases caused by plant pathogenic fungi.

The genus *Fusarium* comprises numerous pathogenic species responsible for a wide array of plant diseases that result in significant economic losses (Nikitin *et al*. 2023). The accurate identification of *Fusarium* species is pivotal for diagnosing and managing associated diseases (O'Donnell *et al*. 2022). The current classification relies on a combination of morphological characteristics and molecular phylogenetic analyses. Commonly utilized genetic sequences used for distinguishing *Fusarium* species include RNA polymerase second largest subunit (*rpb2*) (Laraba *et al*. 2021), translation elongation factor 1-α (*tef1*) (Wulff *et al*. 2010), calmodulin (*CaM*) (O'Donnell *et al*. 2000), β-tubulin (*tub2*) (O'Donnell *et al*. 1998a), as well as internally transcribed spacer regions in the ribosomal repeat region (*ITS1* and *ITS2*) (Waalwijk *et al*. 1996; O'Donnell and Cigelnik 1997). Multi-gene tandem phylogenetic analysis has become a prevalent approach for *Fusarium* species identification. For example, Han *et al*. (2023) employed the *CaM-rpb2-tef1* gene regions to define the *F. oxysporum* species complex (FOSC) among cereal-associated *Fusarium* species in China. Similarly, He *et al*. (2021) utilized multilocus phylogenetic analyses involving sequences of the *ITS*, *tef1*, and *rpb2* genes to identify *F. rosicola* sp. nov., responsible for causing vascular wilt in *Rosa chinensis*.

Between 2021 and 2022, an unclassified wilt disease emerged in a pear orchard located in Nanjing City, Jiangsu Province, China. The symptoms exhibited by this disease are distinct from recognized pear tree diseases and have sporadically appeared in the middle and lower reaches of the Yangtze River, China in recent years. Moreover, a concerning trend of increased incidence and severity is now posing a significant threat to the pear industry. The primary objective of this study was to identify the causal agent responsible for this disease. The fungal isolates obtained were identified as *F. cugenangense* based on both morphological characteristics and phylogenetic analysis. The pathogenicity of the isolated *F. cugenangense* on pear trees was confirmed through artificial inoculation and subsequent reisolation. To observe the infection process, *F. cugenangense* was genetically modified with GFP and visualized using fluorescence microscopy. Notably, the GFP-labeled pathogen initially introduced into the roots was subsequently reisolated from both stems and foliage, providing compelling evidence that this disease exhibits systemic behavior within pear trees.

2. Materials and methods

2.1. Sampling and isolation

Pyrus pyrifolia plants exhibiting symptoms of wilt were collected from Xuanwu District, Nanjing (32°2′17′′N, 118°51′56′′E). Typical disease symptoms were gathered from stems and roots of *P. pyrifolia* and transported to the laboratory. Initially, all samples underwent surface sterilization following the method outlined by Li *et al*. (2020). Subsequently, small sections of necrotic tissue (3 mm×3 mm) from the margins of infected tissues were sterilized using 3% hydrogen peroxide, 75% ethanol, and rinsed with water. These sections were then placed onto potato dextrose agar (PDA) plates and incubated at 25°C for 3 days. Pure cultures were established by transferring a small piece of mycelium from the edge of each colony grown on PDA, followed by single spore isolation, as described by Ma *et al*. (2022).

2.2. Morphological study

Purified strains were inoculated onto PDA plates and incubated at 25°C to observe colony morphology. After 7 days of incubation in the dark on PDA, the cultural characteristics of the colony, including pigmentation, were recorded. Sporulation was induced by culturing in darkness on 1/4 PDA medium for 10 days. Morphological characteristics of microconidia, macroconidia, chlamydospores, and conidiogenous cells were examined and photographed using a Zeiss Axioscope 5 compound microscope equipped with differential interference contrast (DIC) optics. The measurements were conducted using the Zeiss Imaging System software, Zen 3.0 (blue edition, Carl Zeiss Microscopy GmbH, Jena, Germany). A total of 100 microconidia, 50 macroconidia, and 30 chlamydospores were randomly selected for measurement to determine the minimum-maximum ranges and calculate mean values.

2.3. DNA extraction, amplification, and sequencing

Genomic DNA was extracted from fresh fungal mycelium grown on PDA plates using a cetyltrimethylammonium bromide (CTAB) extraction buffer (0.2 mol L^{-1} Tris, 1.4 mol L^{-1} NaCl, 20 mmol L^{-1} EDTA, 0.2 g L^{-1} CTAB), following the protocol described by (He *et al*. 2021). Four gene loci, including *ITS*, *tef1*, *rpb2*, and *CaM*, were amplified using the following primer sets: ITS-1/ITS-4 (Gardes and Bruns 1993), EF1/EF2 (O'Donnell *et al*. 1998b), 5f2/7cr (Reeb *et al*. 2004), and CL1/CL2A (O'Donnell *et al*. 2000). PCRs were carried out using a reaction mixture consisting of 12.5 μL 2× *Taq* PCR Master Mix (Vazyme Biotech Co., Ltd., Nanjing, China), 1 μL each of 10 μmol L^{-1} primers, 1 μL of genomic DNA (approximately 50 ng), and adjusted to a total volume of 25 μL with distilled deionized water. PCR amplifications followed the procedures outlined by Han *et al*. (2023). The resulting PCR products were confirmed by 1% agarose

electrophoresis and subsequently sent to Tsingke Biotech (https://www.tsingke.com.cn/) for Sanger sequencing (Tsingke Biotech, Nanjing, China).

2.4. Phylogenetic analysis

Bayesian inference (BI) methods were used to construct phylogenetic trees for various *Fusarium* species. Combined datasets of *CaM*, *rpb2*, and *tef1* were employed, following dataset construction methods from previous studies (Han *et al*. 2023). Sequences were aligned using Clustal X2 software with default settings and manually optimized within MEGA 7 (https://www.megasoftware.net/). Sequence concatenation was performed using SequenceMatrix (Vaidya *et al*. 2011). The best substitution model (SYM+G) for tree reconstruction was estimated using MrModeltest 2.4 (Nylander 2004). Bayesian inference was conducted in MrBayes v. 3.2.7 (Ronquist *et al*. 2012) with two analyses involving four Markov chains each, running for 1 million generations. Trees were sampled every 1,000th generation, and after discarding the first 25% of trees as the burn-in phase, a consensus Bayesian tree and Bayesian posterior probabilities (BPP) were computed based on the remaining trees. BPP values exceeding 0.95 were considered statistically significant. Tree visualization was carried out using FigTree version 1.4.4 (https://github.com/rambaut/figtree/releases).

2.5. Pathogenicity test

The inoculation method was adapted from He *et al*. (2021) and Soleha *et al*. (2022) with minor refinements. For this investigation, 45-day-old *Pyrus betulaefolia* seedlings, cultivated within the phytotron at Jiangsu Academy of Agricultural Sciences, China, were employed to evaluate pathogenicity. Prior to inoculation, the pear seedlings were carefully extracted from the soil, and their root systems underwent thorough rinsing with distilled water. Subsequently, they were immersed in 100 mL of sterile hydroponic nutrient solution for subsequent usage. Mycelium blocks from the *Fusarium* isolates were introduced into 100 mL of potato dextrose broth (PDB) medium and incubated for 3–5 days at 28°C and 180 r min^{-1} to induce sporulation. Conidia were subsequently harvested and suspended in sterile water at a concentration of 10^8 conidia mL^{-1}. This suspension served as the inoculum, with 200 μL being added to the nutrient solution of 10 test plants, while the uninoculated control received sterile distilled water. This experimental setup was replicated twice. Throughout a 6-week timeframe, the progression of symptoms and the development of the disease were regularly monitored. Observable changes, including wilting and leaf necrosis, were recorded and photographed. Following the observation period, the presence of the pathogen was verified by reisolating it from symptomatic plant tissues. Further confirmation was achieved through the utilization of both morphological and molecular techniques for identification purposes.

2.6. Generation of the GFP-labelled strain

To create the GFP-labelled strain, we employed a polyethylene glycol (PEG)-mediated transformation technique, following the established fungal transformation protocol (Zhou *et al*. 2011). The isolate Pnj-3 was utilized as the parental strain. The plasmid sk1004, harboring the GFP gene regulated by the constitutive promoter GAPDH, was introduced into the fungal strain Pnj-3 through protoplast transformation. The transformed strains were subsequently cultivated on PDA, supplemented with hygromycin B (CalBiochem, La Jolla, CA, USA) at a final concentration of 300 μg mL^{-1}. The successful integration of the GFP gene was confirmed by conducting polymerase chain reaction (PCR) amplification using GFP-specific primers, followed by subsequent gel electrophoresis. To validate GFP expression, fluorescence microscopy (Zeiss Axioscope 5, Carl Zeiss Microscopy, Germany) was utilized to visualize the fluorescence emitted by GFP within hyphal cells. Furthermore, the potential virulence of the GFP-labeled strain was assessed in accordance with Koch's postulates. Tissues from diseased plants were also collected and examined for the colonization of the GFP-labeled fungus using fluorescence microscopy.

2.7. Transmission electron microscopy

To investigate the colonization of *F. cugenangense* within pear tissues using transmission electron microscopy (TEM), stem and leaf sections displaying visible brown lesions were sampled at 15 days post-inoculation (dpi). Each sample was collected from three infected plants and processed according to the method described by Ke *et al*. (2013). Specimens were initially fixed in 4% glutaraldehyde diluted in 0.1 mol L^{-1} phosphate buffer (pH 6.8) overnight, followed by rinsing with the same buffer. Subsequently, they were fixed in 1% osmium tetroxide, dehydrated through a graded series of ethanol, infiltrated with a 3:1, 1:1, 1:3 (v/v) ethanol/LR White resin mixture (London Resin Co., Ltd.), and finally in pure resin. The infiltration time in each mixture was at least 6 h, with 72 h in pure resin. The samples were then embedded in capsules and polymerized at 55°C for 2 days. Ultrathin sections of the samples, cut with a diamond knife, were collected on copper grids for TEM analysis. Following contrast staining with uranyl acetate and lead citrate, the grids were examined using a TEM H-7650 (HITACHI, Japan) operating at 80 kV.

3. Results

3.1. Field observation of the wilt disease in *P. pyrifolia*

In October 2022, an unusual wilt disease appeared in the *P. pyrifolia* Sucui 1 cultivar in Nanjing, China (Fig. 1). The impacted orchard spanned approximately 50 acres, and upon surveying 120 trees, symptoms were observed in 11 cases. Among these, 3 trees succumbed to the disease, 3 exhibited severe symptoms resulting in the death of over half of the branches, while the remaining 5 displayed mild symptoms with noticeable browning at the base of the stems. The disease affected about 10% of the surveyed pear trees. It originated in the roots and gradually moved upwards, causing distinctive browning patterns that spiraled along the tree's vascular tissues (Fig. 1-B–E). The lateral branches of the

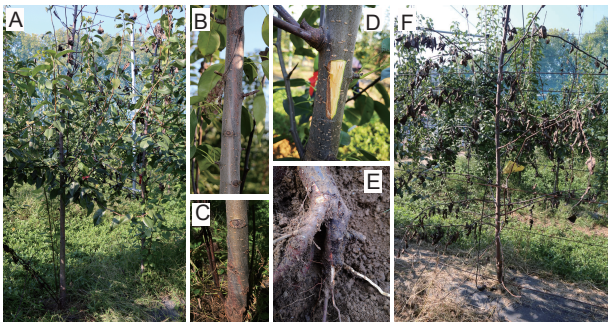


Fig. 1 Natural symptoms of wilt in *Pyrus pyrifolia*. A, a tree in the initial disease stage with several dead branches. B–D, trunk symptoms of afflicted trees. E, root symptoms of the diseased tree. F, late-stage manifestation of withering and death due to the disease.

trunk, emerging from the affected area, displayed severe wilting, eventually resulting in the death of both branches and leaves (Fig. 1-A–D). This insidious progression reached heights of up to two meters above the ground, illustrating its systemic impact on the plant. As the disease advanced, the entire plant exhibited visible wilting symptoms, ultimately leading to its demise (Fig. 1-F). To identify the causative agent of the described field symptoms, we collected samples from both above-ground and below-ground parts of the affected trees for subsequent pathogen isolation.

3.2. Morphological characteristics

Fifteen fungal isolates were successfully retrieved from discolored internal bark tissues sampled from branches, trunks, and roots. Nine isolates were obtained from above-ground stems or branches, while six were retrieved from roots. Among these, 14 isolates exhibited remarkably similar colony and sporulation characteristics, while one was notably distinct and was subsequently excluded as a saprophytic fungus. Colonies cultivated from the 14 isolates on PDA displayed a pale lavender color on their upper surface, while the lower surface exhibited an orange tint adorned with distinctive wheel-like black markings (Fig. 2-A). After 2 weeks of incubation on 1/4 PDA in a dark 25°C environment, a profusion of microconidia was generated, while macroconidia and chlamydospores appeared sporadically (Fig. 2-B and E). Microconidia exhibited an ellipsoidal to cylindrical shape, with variations from straight to curved, 0–2 septa, and measurements falling within the range of 6.6–16.9 μm×2.8–5.6 μm (with an average of 9.9 μm×4.5 μm, *n*=100) (Fig. 2-B and C). On the other hand, macroconidia assumed a falcate shape with terminal foot-like structures, featured 2–5 septa, and measured between 19.2–51.5 μm×3.4–5.1 μm (averaging at 31.2 μm×4.3 μm, *n*=50) (Fig. 2-B and D). Chlamydospores, produced either singly or in pairs at terminal or intercalary positions, exhibited an average diameter ranging from 6.4 to 13.5 μm (mean=9.1 μm, *n*=30) (Fig. 2-E). These morphological characteristics closely resembled those previously described for *F. cugenangense* in studies by Maryani *et al*. (2019), Kim *et al*. (2021) and Yang *et al*. (2023).

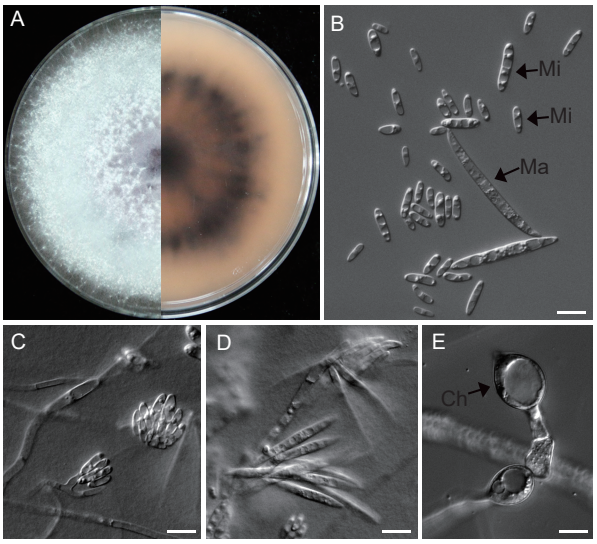


Fig. 2 Morphological features of isolate Pnj-3. A, colony. B, conidia, microconidia (Mi) and marcoconidia (Ma). C and D, conidiogenous cell and conidia on aerial hypha. E, chlamydospores (Ch). Bars=10 μm.

3.3. Molecular identification

For the initial molecular identification, we amplified and sequenced the internal transcribed spacer (*ITS*) sequences of rDNA for these 14 fungal isolates. Sequence alignment revealed identical sequences (GenBank OR649197) among these 14 fungi. Subsequent NCBI BLAST analysis confirmed a 100% sequence identity match with known sequences such as *F. cugenangense* (MW016569), *F. oxysporum* (MN959991), *Fusarium* sp. (MN461531), among others, signifying their classification within the FOSC. To precisely determine the specific species, we sequenced the *CaM*, *rpb2*, and *tef1* genes of two randomly selected isolates, namely Pnj-3 and Pnj-9. Subsequently, these sequences (GenBank OR727356-OR727361) were employed in concatenated multigene phylogenetic analysis. The resulting phylogenetic tree demonstrated a close genetic relationship between these two isolates, Pnj-3 and Pnj-9, and *F. cugenangense* (Fig. 3). Combining the previous morphological characteristics, we identified the obtained isolates as *F. cugenangense*.

3.4. Pathogenicity test

The pathogenicity of three *F. cugenangense* isolates, Pnj-3, Pnj-5, and Pnj-9, was assessed by inoculating healthy *P. betulaefolia* seedlings with a conidia suspension. As depicted in Fig. 4, 4 weeks post-inoculation, plants inoculated with *F. cugenangense* conidia displayed necrotic symptoms reminiscent of those observed in the field. These symptoms included necrosis in the roots, stems, and leaves. In contrast, the control group of plants inoculated with water remained robust and healthy (Fig. 4-A). Notably, the stem of the infected plants exhibited partial necrosis, with the necrotic regions extending upward. Leaves emerging from these affected stem portions turned brown, while those arising from the healthy sections retained their vibrant green color (Fig. 4-B and C). In addition, the roots of the diseased plants exhibited brown

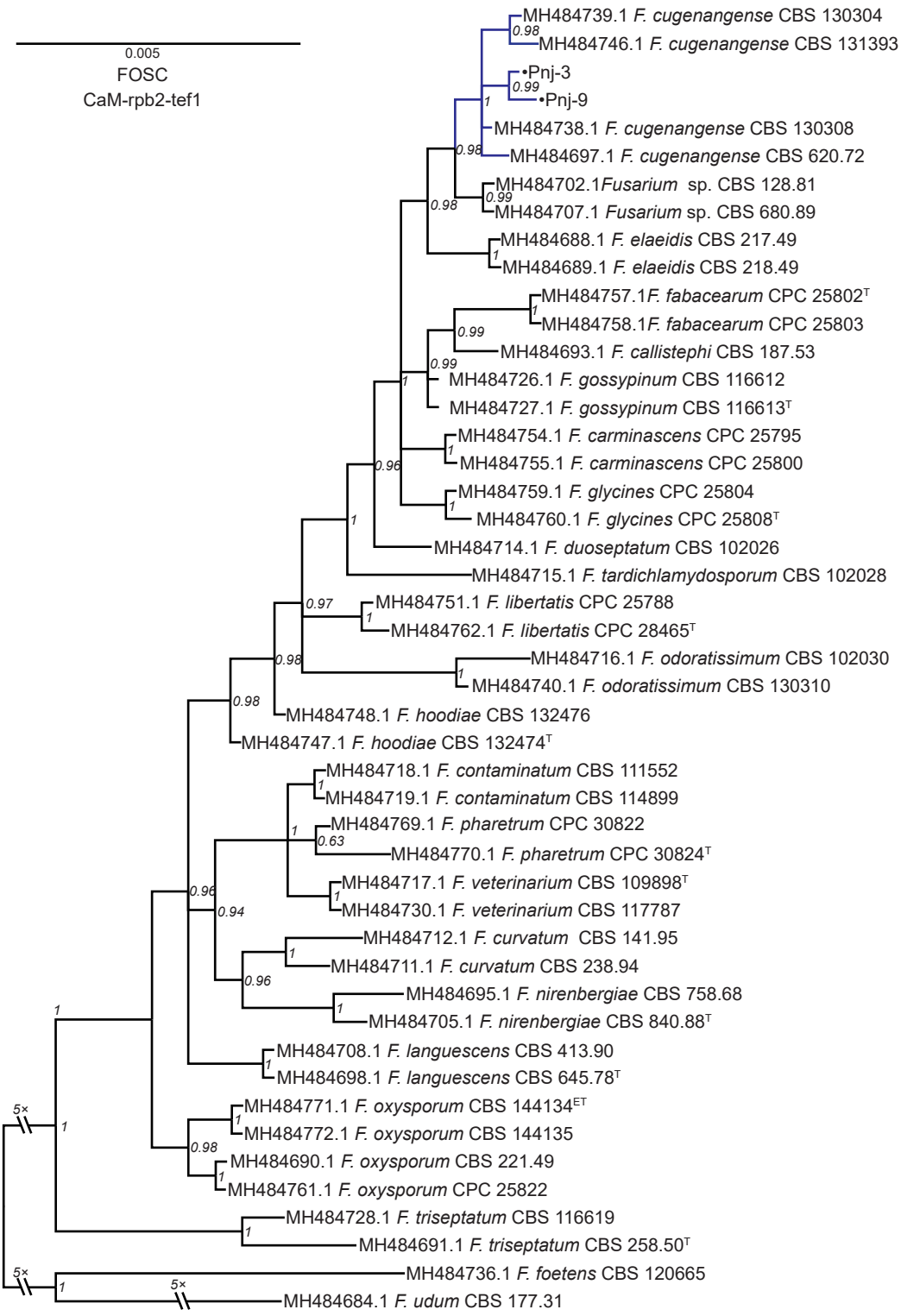


Fig. 3 Phylogeny inferred based on the combined *CaM-rpb2-tef1* gene regions of the *Fusarium oxysporum* species complex (FOSC). *Fusarium udum* (CBS 177.31) was used as an outgroup. Bayesian posterior probabilities (BI-PP>0.9) were displayed at the nodes. Pnj-3 and Pnj-9 were strains isolated in this study. Ex-type and ex-epitype strains were indicated with T and ET, respectively.

discoloration compared to the control plants (Fig. 4-A and B). After 5 weeks, all leaves on the diseased plants exhibited browning symptoms, with some leaves wilting and falling off, pushing the plants to the brink of death (Fig. 4-D–F). This typical necrosis pattern confirmed the virulence of the inoculated *F. cugenangense* isolates. Furthermore, upon re-cultivation from these necrotic regions, the fungal colonies, aerial mycelia, and conidia displayed morphological traits highly consistent with those of the original isolate, further substantiating the pathogenic identity of *F. cugenangense* isolates.

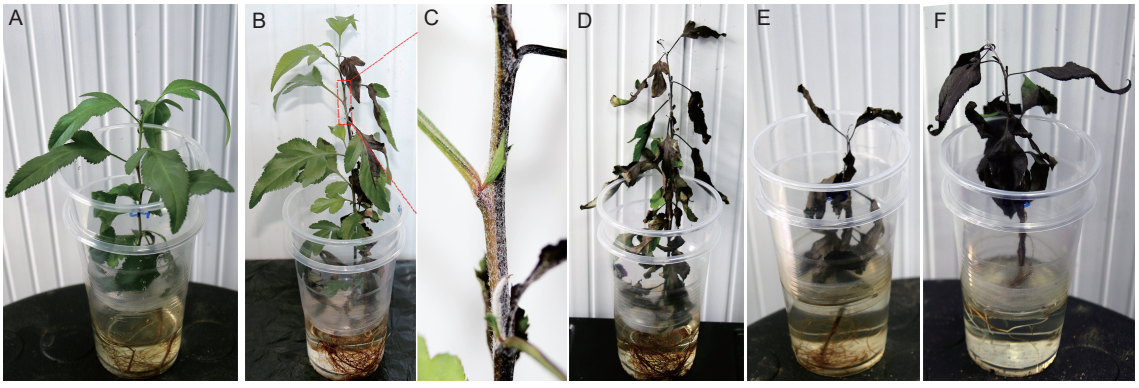


Fig. 4 Pathogenicity assessment of *Fusarium cugenangense* isolates on hydroponically grown *Pyrus betulaefolia* seedlings. A, control plant 4 weeks post-inoculation. B and C, localized necrotic symptoms observed on Pnj-3 inoculated plants four weeks post-inoculation. D–F, complete plant wilting and signs of death observed after 5 weeks post-inoculation with Pnj-3, Pnj-5, and Pnj-9, respectively.

3.5. Invasive growth of *F. cugenangens* on pear plant tissue

A substantial proportion of plants did not exhibit disease symptoms in their stems and leaves after being inoculated with *F. cugenangens* conidia. To gain deeper insights into the infection process, we engineered a strain of *F. cugenangens* expressing GFP fluorescence. As illustrated in Fig. 5-A, this genetically modified strain effectively expressed the GFP protein at both the spore and hyphal stages, allowing us to consistently monitor spore and hyphae growth locations through fluorescence microscopy. One-week post-inoculation, we examined root tissues and observed fluorescence-labeled *F. cugenangens* strains initiating germination in pear root tissues and invading root epidermal cells (Fig. 5-B). After an additional month of cultivation, during which some plants exhibited necrotic symptoms in stems and leaves, we dissected stem and leaf tissues. Our examination revealed that fluorescence-labeled hyphae had colonized plant tissues displaying browning symptoms. Remarkably, hyphae in stem tissues exhibited a preference for longitudinal extension, while in leaf vein tissues, they closely adhered to vein patterns (Fig. 5-C–E). Within leaf mesophyll cells, the invading hyphae exhibited an irregular growth pattern (Fig. 5-F). After sectioning the stems and leaves of diseased plants into ultrathin slices, we also observed the presence of fungal hyphae within the plant tissues. As shown in Fig. 6, cross-sections of fungal hyphae were observed within the vascular bundles of both the stems and leaf veins. Fungal hyphae were evident in the intercellular spaces as well as inside the plant cells. These observations collectively affirm *F. cugenangens*' capacity to infect pear root cells and its inclination for upward extension from the roots, subsequently inducing systemic disease symptoms.

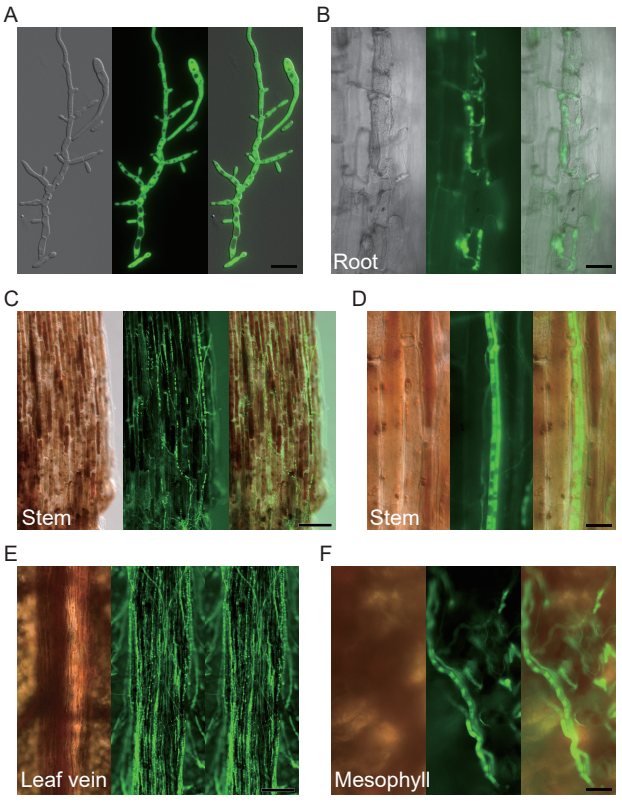


Fig. 5 Infection process of GFP-labeled *Fusarium cugenangens*. A, GFP labeling of the fungal pathogen. B, examination of invasive hyphae in diseased pear root tissues. C and D, observation of invasive hyphae in pear stem tissues. E, observation of invasive hyphae in pear leaf veins. F, observation of invasive hyphae in pear leaf mesophyll cells. Scale bars represent 20 μm in (A), (B), (D), and (F), while 100 μm in panels (C) and (E).

4. Discussion

Fusarium cugenangense belongs to the FOSC, a group renowned for its involvement in various plant diseases. Typically, these complex members induce vascular wilts, but they can also be responsible for root and bulb rots. The presence of *F. cugenangense* was initially reported based on phylogenetic and genetic diversity analyses of the banana *Fusarium* wilt pathogen in Indonesia (Maryani *et al*. 2019). Furthermore, this pathogen has been documented to cause diseases in a variety of plant species, including *Acer palmatum*, *Crocus* sp., *Gossypium barbadense*, *Hordeum vulgare*, *Solanum tuberosum*, *Smilax* sp., *Tulipa gesneriana*, *Musa nana*, *Musa* sp., *Vicia faba*, *Zea mays* and *Camellia sinensis* (Maryani *et al*. 2019; Wang *et al*.

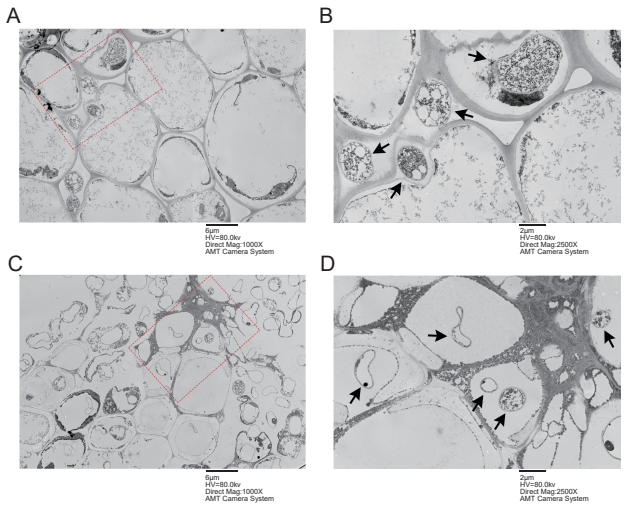


Fig. 6 Transmission electron micrographs of pear plant cells colonized by fungal hyphae of *Fusarium cugenangens*. A and B, fungal hyphae observed in intercellular and intracellular spaces of infected stem tissue. C and D, fungal hyphae observed in vascular bundle cells of leaf veins. A and C are magnified 1,000×, with a scale bar of 6 μm. B and D represent the regions outlined in red boxes in A and C, magnified at 2,500×, with a scale bar of 2 μm. Fungal hyphae are marked with arrows.

2022; Han *et al*. 2023; Yang *et al*. 2023). In this study, we identified *F*. *cugenangense* as the causative agent of the newly emerging pear tree wilt disease in the Nanjing region using traditional morphological characteristics and molecular phylogenetic analysis. To our knowledge, this is the first report of *F*. *cugenangense* affecting pear production in China.

Accurate species-level identification of a causative agent is vital for disease diagnosis and management, associating it with established knowledge of host ranges, geographic distributions, and toxin production potentials (O'Donnell *et al*. 2022). Nonetheless, the taxonomic classification of *Fusarium* species presents several challenges due to factors such as the impact of environmental conditions on morphological characteristics, limitations of the internal transcribed spacer region (ITS) as a universal barcode for fungi, and inaccuracies in species and genus names within public databases (Aoki *et al*. 2014; Lombard *et al*. 2019; Han *et al*. 2023). To overcome these challenges, a phylogenomic approach has been employed to redefine generic boundaries (Geiser *et al*. 2021). Recently, the phylogenomic approach has been increasingly recognized for its ability to provide valuable insights into species evolution and boundaries (Liu *et al*. 2022; Wang *et al*. 2022; Han *et al*. 2023). Building upon the multi-gene methodology utilized by Han *et al*. (2023) to accurately identify pathogens of the FOSC in Chinese cereal crops, this study adopted *CaM*, *rpb2*, and *tef1* gene sequences for phylogenetic reconstruction, definitively confirming *F*. *cugenangense* as the species responsible for the wilt symptoms in Chinese pear trees.

Among the common pathogenic fungi, genera like *Rhizoctonia*, *Phytophthora*, and *Pythium* are notorious for triggering root rot in pear trees (Wang *et al*. 2013; Williamson-Benavides and Dhingra 2021). The symptoms of pear tree root rot may vary depending on the specific pear cultivar and environmental conditions (Sardella *et al*. 2016). However, infected pear trees typically exhibit growth retardation, leaf yellowing, leaf abscission, and an overall decline in vitality (Wang *et al*. 2013). In this study, we unveiled a new disease symptom caused by *F*. *cugenangense* that differs from the symptoms of other known pear root diseases. Infected pear trees exhibit symptoms that extend from the base of the trunk upwards in a spiraling pattern, uninterrupted, and in some cases, reaching a height of more than two meters above ground. Additionally, our observations of fluorescently labeled invasive hyphae in stem tissues revealed a longitudinal extension pattern, which may elucidate the upward progression of diseased tree bark. To the best of our knowledge, this new symptom has not been reported in other pear diseases, making it a distinguishing feature for rapid field identification of this disease. Limited reports currently exist on the symptomatology of *F*. *cugenangense* on other host crops. For instance, *Fusarium* wilt in Korean blackberry leads to leaf wilting, stem darkening, and eventual plant blight (Kim *et al*. 2021). Likewise, affected tea plants exhibit symptoms ranging from leaf wilting to complete death, with characteristic black lesions and root rot associated with this disease (Yang *et al*. 2023). These documented symptoms do not resemble the novel observations we described on the affected pear tree trunks in this study.

The initial stage of plant host colonization typically involves spore germination, although this process can be inhibited by fungistasis (Garbeva *et al*. 2011). Fungal spores can overcome fungistasis when an external nutrient source is available, such as plant root exudates (Gordon 2017). In this study, with the aid of fluorescence microscopy, we were able to observe spore germination on the root cells of all experimental pear seedlings. However, during subsequent cultivation, we observed that the infection rate for systemic symptoms in pear trees inoculated with *F*. *cugenangense* ranged between 30–60%. These findings suggest that although pear seedling root exudates can induce *F*. *cugenangense* spore germination, other factors may influence the pathogen's ability to establish systemic infections. As noted by Gordon (2017), these additional factors encompass the quantity and composition of root exudates, the structural characteristics of the plant hypodermis, and the response of cortical tissue and the endodermis to a pathogen's invasive growth. In pear plants exhibiting systemic symptoms, we observed GFP-labeled *F*. *cugenangense* strains in root, stem, and leaf tissues, thereby confirming *F*. *cugenangense* as the causative agent of pear tree wilting symptoms.

Root diseases represent a substantial threat to fruit tree health and productivity, leading to reduced yields and overall decline of orchard health. Although the incidence of this wilt disease within our germplasm resource garden remains relatively low, with rates not exceeding 10% in the surveyed area, it is essential to underscore that, in most instances, its occurrence leads to tree mortality, resulting in significant economic losses. Furthermore, similar symptoms have been mentioned by orchard owners or local technicians in the Yangtze River region, although sample data and statistics

from other areas are currently unavailable. Additionally, this disease has a tendency to spread to neighboring trees, persisting even after the removal of affected ones. Therefore, the threat posed by *F. cugenangense* in the Yangtze River region remains a matter of concern, warranting further attention to prevent larger-scale losses. This study not only identifies the pathogen responsible for the disease but also provides a detailed description of the symptoms it causes. These research findings will be valuable for the identification, diagnosis, and formulation of targeted control measures for this newly emerging pear wilt disease.

5. Conclusion

In this study, we have documented the emergence of a novel pear disease caused by *F. cugenangense*. The pathogen's identity was confirmed through a comprehensive approach involving morphological examination, multigene phylogenetic analysis, and Koch's postulate. The pathogen's identification and the detailed symptom presentation presented in this study will serve as invaluable references for pear-producing regions globally. This information will aid in disease identification, symptom recognition, and the development of targeted control measures. Our future research endeavors will focus on investigating the resistance of commonly used pear rootstocks to *F. cugenangense* and screening for effective fungicides against this pathogen.

Acknowledgements

This work was supported by the Jiangsu Agricultural Science and Technology Innovation Fund, China (CX(23)1011), the Earmarked Fund for China Agriculture Research System (CARS-28), the National Natural Science Foundation of China (31901837), the China Postdoctoral Science Foundation (2020M671389), the Basal Research Fund for the Jiangsu Academy of Agricultural Sciences, China (ZX(23)3016), and the Yafu Technology Service Project, China (KF(23)1106).

Declaration of competing interest

The authors declare that they have no conflict of interest.

Declaration of generative AI and AI-assisted technologies in the writing process

The authors declare that they did not use AI in the preparation and writing of this manuscript.

References

Aoki T, O'Donnell K, Geiser D M. 2014. Systematics of key phytopathogenic *Fusarium* species: Current status and future challenges. *Journal of General Plant Pathology*, **80**, 189–201.

Bodah E T. 2017. Root rot diseases in plants: A review of common causal agents and management strategies. *Agricultural Research & Technology: Open Access Journal*, **5**, 555661.

Garbeva P, Hol W G, Termorshuizen A J, Kowalchuk G A, De Boer W. 2011. Fungistasis and general soil biostasis — a new synthesis. *Soil Biology and Biochemistry*, **43**, 469–477.

Gardes M, Bruns T D. 1993. ITS primers with enhanced specificity for basidiomycetes — Application to the identification of mycorrhizae and rusts. *Molecular Ecology*, **2**, 113–118.

Geiser D M, Al-Hatmi A M, Aoki T, Arie T, Balmas V, Barnes I, Bergstrom G C, Bhattacharyya M K, Blomquist C L, Bowden R L. 2021. Phylogenomic analysis of a 55.1-kb 19-gene dataset resolves a monophyletic *Fusarium* that includes the *Fusarium solani* species complex. *Phytopathology*, **111**, 1064–1079.

Gordon T R. 2017. *Fusarium oxysporum* and the *Fusarium* Wilt Syndrome. *Annual Review of Phytopathology*, **55**, 23–39.

Han S L, Wang M M, Ma Z Y, Raza M, Zhao P, Liang J M, Gao M, Li Y J, Wang J W, Hu D M, Cai L. 2023. *Fusarium* diversity associated with diseased cereals in China, with an updated phylogenomic assessment of the genus. *Studies in Mycology*, **104**, 87–148.

He J, Li D W, Zhang Y, Ju Y W, Huang L. 2021. *Fusarium rosicola* sp. nov. causing vascular wilt on *Rosa chinensis*. *Plant Pathology*, **70**, 2062–2073.

Ke X, Huang L, Han Q, Gao X, Kang Z. 2013. Histological and cytological investigations of the infection and colonization of apple bark by *Valsa mali* var. *mali*. *Australasian Plant Pathology*, **42**, 85–93.

Kim W G, Choi H W, Park G S, Cho W D. 2021. *Fusarium* wilt of korean blackberry caused by *Fusarium cugenangense*. *Research in Plant Disease*, **27**, 187–191.

Laraba I, McCormick S P, Vaughan M M, Geiser D M, O'Donnell K. 2021. Phylogenetic diversity, trichothecene potential, and pathogenicity within *Fusarium sambucinum* species complex. *PLoS ONE*, **16**, e0245037.

Li C, Jia Y, Tian Y, Zhou L, Sun W, Deng J, Liu F. 2020. First report of necrotic disease caused by *Pantoea agglomerans* on plum (*Prunus salicina*) in China. *Plant Disease*, **104**, 1248.

Liu F, Ma Z, Hou L, Diao Y, Wu W, Damm U, Song S, Cai L. 2022. Updating species diversity of *Colletotrichum*, with a phylogenomic overview. *Studies in Mycology*, **101**, 1–56.

Lombard L, Sandoval-Denis M, Lamprecht S C, Crous P W. 2019. Epitypification of *Fusarium oxysporum*-clearing the taxonomic chaos. *Persoonia*, **43**, 1–47.

Ma X Y, Jiao W Q, Li H, Zhang W, Ren W C, Wu Y, Zhang Z C, Li B H, Zhou S Y. 2022. *Neopestalotiopsis eucalypti*, a causal agent of grapevine shoot rot in cutting nurseries in China. *Journal of Integrative Agriculture*, **21**, 3684–3691.

Maryani N, Lombard L, Poerba Y S, Subandiyah S, Crous P W, Kema G H J. 2019. Phylogeny and genetic diversity of the banana *Fusarium* wilt pathogen *Fusarium oxysporum* f. sp. *cubense* in the Indonesian centre of origin. *Studies in Mycology*, **92**, 155–194.

Nikitin D A, Ivanova E A, Semenov M V, Zhelezova A D, Ksenofontova N A, Tkhakakhova A K, Kholodov V A. 2023. Diversity, ecological characteristics and identification of some problematic phytopathogenic *Fusarium* in soil: A review. *Diversity*, **15**, 49.

Nylander J. 2004. MrModeltest ver. 2. Evolutionary Biology Centre, Uppsala University, Sweden.

O'Donnell K, Cigelnik E. 1997. Two divergent intragenomic rDNA ITS2 types within a monophyletic lineage of the fungus *Fusarium* are nonorthologous. *Molecular Phylogenetics and Evolution*, **7**, 103–116.

O'Donnell K, Cigelnik E, Nirenberg H I. 1998a. Molecular systematics and phylogeography of the *Gibberella fujikuroi* species complex. *Mycologia*, **90**, 465–493.

O'Donnell K, Kistler H C, Cigelnik E, Ploetz R C. 1998b. Multiple evolutionary origins of the fungus causing Panama disease of banana: Concordant evidence from nuclear and mitochondrial gene genealogies. *Proceedings of the National Academy of Sciences of the United States of America*, **95**, 2044–2049.

O'Donnell K, Nirenberg H I, Aoki T, Cigelnik E. 2000. A multigene phylogeny of the *Gibberella fujikuroi* species complex: Detection of additional phylogenetically distinct species. *Mycoscience*, **41**, 61–78.

O'Donnell K, Whitaker B K, Laraba I, Proctor R H, Brown D W, Broders K, Kim H S, McCormick S P, Busman M, Aoki T, Torres-Cruz T J, Geiser D M. 2022. DNA sequence-based identification of *Fusarium*: A work in progress. *Plant Disease*, **106**, 1597–1609.

Reeb V, Lutzoni F, Roux C. 2004. Contribution of RPB2 to multilocus phylogenetic studies of the euascomycetes (Pezizomycotina, Fungi) with special emphasis on the lichen-forming Acarosporaceae and evolution of polyspory. *Molecular Phylogenetics and Evolution*, **32**, 1036–1060.

Ronquist F, Teslenko M, van der Mark P, Ayres D L, Darling A, Höhna S, Larget B, Liu L, Suchard M A, Huelsenbeck J P. 2012. MrBayes 3.2: Efficient bayesian phylogenetic inference and model choice across a large model space. *Systematic Biology*, **61**, 539–542.

Sardella D, Muscat A, Brincat J P, Gatt R, Decelis S, Valdramidis V. 2016. A comprehensive review of the pear fungal diseases.

International Journal of Fruit Science, **16**, 351–377.
Soleha S, Muslim A, Suwandi S, Kadir S, Pratama R. 2022. The identification and pathogenicity of *Fusarium oxysporum* causing acacia seedling wilt disease. *Journal of Forestry Research*, **33**, 711–719.
Sun M, Zhang M, Kumar S, Qin M, Liu Y, Wang R, Qi K, Zhang S, Chang W, Li J, Wu J. 2023. Genomic selection of eight fruit traits in pear. *Horticultural Plant Journal*, **10**, 318–326.
Türkölmez Ş, Çiftçi O, Derviş S, Serçe Ç. 2016. First report of *Phytophthora palmivora* causing crown and root rot on pear (*Pyrus communis*) trees in Turkey. *Plant Disease*, **100**, 519.
Vaidya G, Lohman D J, Meier R. 2011. SequenceMatrix: Concatenation software for the fast assembly of multi-gene datasets with character set and codon information. *Cladistics*, **27**, 171–180.
Waalwijk C, de Koning J R, Baayen R P, Gams W. 1996. Discordant groupings of *Fusarium* spp. from sections Elegans, Liseola and Dlaminia based on ribosomal ITS1 and ITS2 sequences. *Mycologia*, **88**, 361–368.
Wang G, Hong N, Wang J. 2013. Pear root diseases caused by fungi. In: Zhang S, ed., *Pear Study*. China Agriculture Press, China. pp. 590–592.
Wang M, Crous P W, Sandoval-Denis M, Han S L, Liu F, Liang J, Duan W, Cai L. 2022. *Fusarium* and allied genera from China: Species diversity and distribution. *Persoonia — Molecular Phylogeny and Evolution of Fungi*, **48**, 1–53.
Williamson-Benavides B A, Dhingra A. 2021. Understanding root rot disease in agricultural crops. *Horticulturae*, **7**, 33.
Wu J, Wang Y, Xu J, Korban S S, Fei Z, Tao S, Ming R, Tai S, Khan A M, Postman J D, Gu C, Yin H, Zheng D, Qi K, Li Y, Wang R, Deng C H, Kumar S, Chagne D, Li X, *et al.* 2018. Diversification and independent domestication of Asian and European pears. *Genome Biology*, **19**, 77.
Wulff E G, Sorensen J L, Lubeck M, Nielsen K F, Thrane U, Torp J. 2010. Fusarium spp. associated with rice Bakanae: Ecology, genetic diversity, pathogenicity and toxigenicity. *Environmental Microbiology*, **12**, 649–657.
Yang Y, Yang X, Zhang Y, Ren Z, Zhong J, Hu Q, Tan L. 2023. First report of *Fusarium cugenangense* causing root rot of tea plants (*Camellia sinensis*) in China. *Plant Disease*, **108**, 214.
Zhou X, Li G, Xu J R. 2011. Efficient approaches for generating GFP fusion and epitope-tagging constructs in filamentous fungi. *Methods in Molecular Biology*, **722**, 199–212.
Zhu L W, Tang X M, Lin T Y, Zhou S S, Liu P, Ye Z F, Wang D S, Wu Z Y. 2017. First report of *Fusarium* root rot in Asian pear caused by *Fusarium solani* in China. *Plant Disease*, **101**, 252.

Executive Editor-in-Chief Fanghao Wan
Managing Editor Juan Zhang